J Mater Sci (2015) 50:2459–2466
DOI 10.1007/s10853-014-8801-3

Synergistic effect of vegetable protein and silicon addition on geopolymeric foams properties

Letizia Verdolotti · Barbara Liguori · Ilaria Capasso · Agostino Errico · Domenico Caputo · Marino Lavorgna · Salvatore Iannace

Received: 23 October 2014 / Accepted: 16 December 2014 / Published online: 30 December 2014

Abstract Organic–inorganic hybrid foams based on an alkali alumino-silicate matrix were prepared using different foaming methods. Firstly, silico-aluminate inorganic matrix, activated through a sodium silicate solution, was prepared at room temperature. The obtained viscous paste was expanded by means of silicon metal redox reaction in alkaline media in combination with protein-assisted foaming. The foamed systems were hardened at defined temperature and time and then characterized by FTIR, scanning electron microscopy, and compression tests. The high temperature behavior and specific surface area were also evaluated. The experimental findings highlighted that the combination of silicon metal and vegetable protein allowed tailoring hybrid foams with enhanced properties: good yield strength and thermal resistance typical of geopolymeric foam with a ductile behavior (toughness) and low density typical of organic foams.

L. Verdolotti · A. Errico · M. Lavorgna · S. Iannace
Institute for Polymers, Composites and Biomaterials, National Research Council, Naples, Italy

B. Liguori (✉) · I. Capasso · D. Caputo
Department of Chemical, Materials and Industrial Production Engineering, University of Naples Federico II, P.le Tecchio, 80, 80125 Naples, Italy
e-mail: barbara.liguori@unina.it

S. Iannace
IMAST SCRAL, Piazza Bovio 22, 80133 Naples, Italy

Introduction

Inorganic polymer, widely known as geopolymer materials, due to their high early strength as well as good fire resistance and thermal insulation is currently attracting great interest in the production of foams for use as insulating materials in high performance applications (such as transport and aerospace) [1–3]. These materials are produced by reacting an alumino-silicate powder with a highly concentrated aqueous alkali hydroxide and/or silicate solution with the production of a synthetic amorphous-to-semi-crystalline alkali alumino-silicate new phase. The chemical mechanisms involved during this process provide the formation of an intrinsically nanoporous material, characterized by nano-particulates ranging from 5 to 15 nm, and nano-pores of 3–10 nm. In situ inorganic foaming approaches allow tailoring the cellular structure of the alkali-activated materials in the meso to macro range. In this respect, different foaming procedures based on gas evolution in the viscous matrix have been widely exploited. Some authors proposed the hydrogen peroxide (H_2O_2) as chemical blowing agent for the foaming of the geopolymeric pastes [4, 5]. In fact, H_2O_2 is thermodynamically unstable, and therefore it can be easily decomposed to water and oxygen gas with the latter playing the role of the blowing agent:

$$2H_2O_2 \rightarrow 2H_2O + O_2.$$

Another chemical foaming process is based on the redox reaction of Al or Si, in alkaline solution, which induces porosity by H_2 evolution [2, 6–8]. For many industrial applications, it is essential to have foams of cellular morphology in terms of controlling the pore structure (shape, morphology and orientation) as well as texture, total porosity, and pore size distribution [9]. These properties are strongly affected by the foam stability of the viscous system before hardening or gelation.

Proteins have been often proposed to stabilize different kind of foams and emulsions, since their active surface can lower the interfacial tension of fluid interfaces [10, 11]. Recently, proteins have been used in cellular concrete as agent to reduce the surface tension of the solution and stabilize air bubbles embedded in the matrix through a mixing operation. The protein molecules adsorb at the interface between air and water via hydrophobic areas, and a partial unfolding (i.e., surface denaturation) occurs which contributes to stabilize the air bubbles [12–15].

In our knowledge, the simultaneous use of "in situ" chemical foaming and protein-assisted foaming has never been proposed and it can be considered an innovative approach to tailor the chemical–physical properties and density of inorganic foaming.

In this paper, we investigated the effect of a chemical blowing agent such as silicon metal redox reaction in alkaline media in combination with a protein-assisted foaming on the density and mechanical properties of geopolymeric foam. Moreover, the effects of the foaming procedures as well as the chemical composition on the cellular morphology and chemical properties were also analyzed.

Experimental: materials and methods

Materials

The Sodium Silicate (SS) (Na_2O 8.15 %, SiO_2 27.40 %) was provided by Prochin Italia Srl; the silico-aluminate powder (MK) was provided by BASF with the following composition: Al_2O_3 42 wt%; SiO_2 53 wt%; K_2O 0.60 wt%; Fe_2O_3 1.70 wt%; TiO_2 1.83 wt%; MgO 0.50 wt%; CaO 0.37 wt%. Si metal powder and Na_2SiF_6 catalyst were purchased by Merck and Sigma-Aldrich, respectively. Vegetable protein in water solution (pH 7) was supplied by Isolchem s.r.l. Italia.

Design of geopolymeric foams

In order to control the morphology and porosity of the geopolymeric foams, the kinetic of the following chemical–physical reactions was evaluated.

Geopolymer formation

This complex process involves the dissolution of silico-aluminate amorphous phases in contact with high pH alkaline solutions (i.e., sodium silicate). In particular, both SiO_4 and AlO_4 units, released from the amorphous phase reorient and polycondense leading to a strong network, which provides interparticle bonding and physical strength of geopolymer [16]. The schematic formation of a geopolymer can be illustrated by the following reactions [17]:

(geopolymer precursors)

$$n(Si_2O_5, Al_2O_2) + 2nSiO_2 + 4nH_2O + NaOH/KOH \rightarrow Na^+, K^+ + n(OH)_3\text{-}Si\text{-}Al^-(OH)_2\text{-}O\text{-}Si\text{-}(OH)_3 \quad (1) \qquad (1)$$

(geopolymer backbone)

$$n(OH)_3\text{-}Si\text{-}Al^-(OH)_2\text{-}O\text{-}Si\text{-}(OH)_3 + NaOH/KOH \rightarrow (Na^+, K^+)\text{-}(\text{-}Si\text{-}O\text{-}Al^-\text{-}O\text{-}Si\text{-}O\text{-}) + 4nH_2O \qquad (2)$$

Simultaneously to the dissolution, the Sodium Silicate (SS) solution condenses to form a silica gel $[(SiO_2)_n 2n(H_2O)]$, which evolves in a glassy material $[(SiO_2)_n]$. This mechanism is based on the following reactions. The SS consists of a water solution of alkaline silica made of silicic acid:

$$SiO_2/Na_2O + 3H_2O \Leftrightarrow 2NaOH + Si(OH)_4. \qquad (3)$$

The addition of a specific catalytic acid additive, Na_2SiF_6, allows to control the gel's formation of the SS solution. In fact, Na_2SiF_6, in alkaline solution at 40 °C gives SiF_6^{2-} ions, which have an acid hydrolysis as follow [18]:

$$SiF_6^{2-} + (n+2)\ H_2O \Leftrightarrow SiO_2 * nH_2O + 6F^- + 4H^+. \qquad (4)$$

The catalyst affects the equilibrium reaction (Eq. 3) promoting the formation of silicic acid ($Si(OH)_4$) and consequently

the gelification of the system. Even though either the content of silicic acid or the condensation reactions allow the formation of a network with high crosslinking degree (Eq. 5):

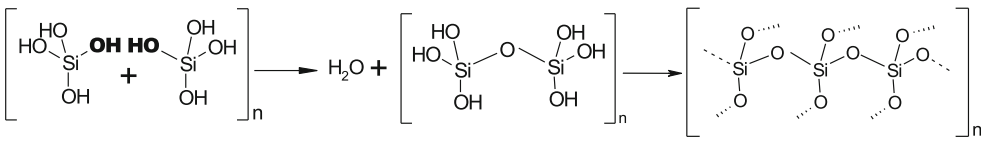

(5)

The amount of catalyst and its typology have a key role on both setting time and mechanical characteristics of the final glassy material.

Foaming processes

This step can be obtained by several mechanisms:

(1) Chemical foaming: this process is obtained by gaseous hydrogen, H_2, produced through the redox reaction of Si powder in the alkaline media [19]:

$$Si + 4H_2O \rightarrow 2H_2 + Si(OH)_4. \quad (6)$$

(2) Protein foaming: this process, usually employed in porous ceramic materials production, consists in a strongly whipping of the vegetable protein that, added to the inorganic mixture, can act as "*meringue*" type foam. Since the rate of whipping influences strongly the expansion grade, it has to be suitably selected, in order to obtain a stable foam network, able to maintain itself during the gelling and consolidation processes.

In order to allow the entrapping of the bubbles in the geopolymeric matrix, the foaming step has to take place just before the gelification of the system.

Finally, it was taken into account that all the above reactions are strongly influenced by curing conditions such as time, temperature, and relative humidity.

Preparation of geopolymeric foams

Three different hybrid foams based on a starting mixture of 70 % wt. SS, 8.7 % wt. Na_2SiF_6, and 21.3 % wt. silicoaluminate source (MK), were prepared. In particular, the first foam (SCF) was prepared by mixing 8 wt% of Si powder to the SS solution for 1 h, and subsequently the other materials were added and homogeneously mixed. The second foam (PCF) was prepared by adding to the starting mixture 12 wt% of a "meringue" type foam, obtained from an aqueous solution containing a mixture of vegetable proteins. The "*meringue*" was prepared using an Ultra-Turrax disperser at 12000 rpm up to obtain a volume 8 times the initial one. The third foam (HCF) was prepared using simultaneously the Si powder and whipped protein. The composition of each geopolymeric foam is summarized in Table 1.

The slurries (namely SCF, HCF, and PCF) were cast in plastic prismatic (4 × 4 × 16 mm) open molds and cured at 40 °C for 24 h at room humidity. It has been proved that prolonging the curing time and increasing the curing temperature (up to 60 °C) can speed up the harden process and improve the physical properties of a geopolymer sample. However, curing at too high temperatures (80 and 10 °C) or for longer time (more than 72 h) do not provide any significant improvement in chemical and mechanical properties [20].

Therefore, after curing, foams were let at 60 °C in hydrothermal conditions (100 % Relative Humidity) for 72 h (namely *h*-SCF, *h*-HCF, and *h*-PCF).

Characterization of geopolymeric foams

The cellular morphology of the hybrid foams was examined by SEM (SEM, Cambridge S440) and image (Image J®) analysis was performed in order to assess the pore structure of foamed systems. The samples were cross-sectioned, gold sputtered, and analyzed at an accelerating voltage of 20 kV. For the image analysis, the SEM micrographs were converted to 8-bit digital images prior to be analyzed by the

Table 1 Geopolymeric foam mixtures composition

Geopolymeric foam	Starting mixture (wt%)			Foaming agent addition (wt%[a])	
	SS	MK	Na_2SiF_6	Si	Protein
SCF	70	21.3	8.7	8	No
PCF	70	21.3	8.7	No	12
HCF	70	21.3	8.7	8	12

[a] wt% is referred to the starting mixture

Image J® software in order to evaluate the pore size distributions and the mean pore size (ASTM D3576).

The chemical modifications that occur in the system during the formation of geopolymeric foam were evaluated by FTIR spectroscopy. FTIR spectra were collected at room temperature using a Nicolet apparatus (Thermo Scientific, Italy) from 4000 to 600 cm^{-1} with a wavenumber resolution of 4 cm^{-1} for 64 scans. The FTIR spectra were collected in absorbance mode on transparent pellets obtained by dispersing the sample in the form of powder in KBr (2 wt%).

Flexural and compressive tests were carried out on the above described prismatic samples using a SANS testing machine (mod. CMT4304, Shenzhen SANS Testing Machine Co., China) with a 30 kN load cell, according to ASTM D1621 and a loading rate of 2 mm/min. The density was calculated as the ratio between the foam weight (as measured with an analytical balance) and the geometrical volume. All the tests were performed in triplicate.

N_2 adsorption/desorption analysis was carried out at 77 K using a Micromeritics ASAP 2020. Specific surface areas were evaluated using the BET method.

Results and discussion

The morphological properties and the pore size distributions of each foam are shown in Fig. 1. In Fig. 1a, a cellular structure with a large number of closed cells having a size distribution ranging from 70 μm to 350μm for SCF system was observed. This morphology confirms that the hydrogen produced during the redox reaction of the Si powder generates a cellular structure within the inorganic matrix.

A different morphology was observed in PCF foams (Fig. 1b). Here the foamed structured was characterized by

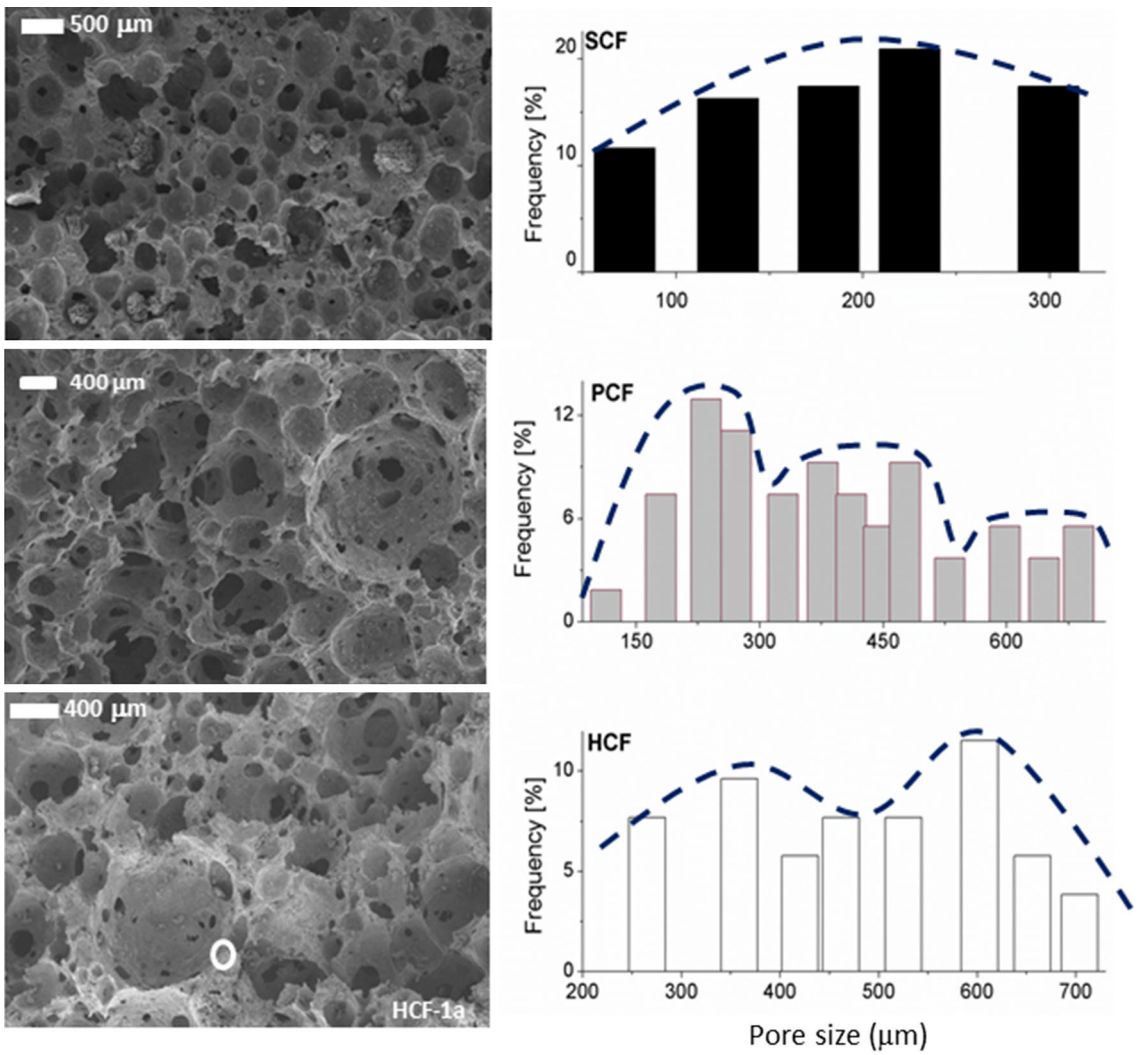

Fig. 1 Morphological characteristic and pore size distribution of each foam

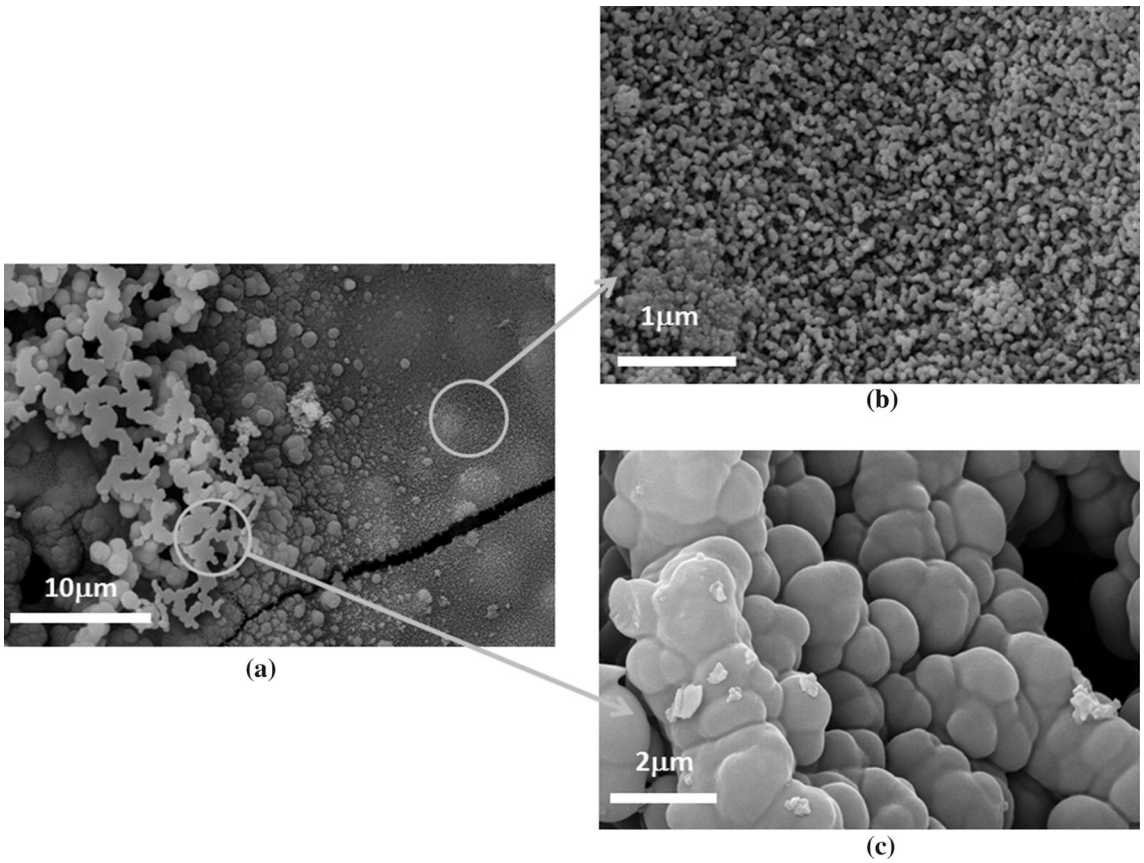

Fig. 2 SEM images of HCF at **a** 7000×, **b** 64000× and **c** 29000×

a non-homogeneous microstructure with the presence of a large amount of open cells.

Figure 1c shows the morphology of HCF foam. The cellular morphology of the foam is characterized by an open-cell structure with an interconnected porosity and a pore size distribution that increased up to 200–700 μm.

At higher magnification (Fig. 2a), the presence of different inorganic structures located in the cell walls of HCF was shown (enlargement of the white circle in Fig 1c). In particular, it is possible to distinguish the geopolymeric nano-precipitates (Fig. 2b) resulting from the reaction of silico-aluminate source in silicate solution media, and some un-reacted silico-aluminate particles (Fig. 2c) [21, 22].

Figure 3 shows the FTIR spectra of MK, SCF, HCF, PCF, *h*-SCF, and *h*-HCF. The MK shows a broad absorption band centered at 1069 cm^{-1} frequency assigned to the overlapping of T–O–Si (T = Si or Al) asymmetric stretching peaks typical of alumino-silicate species [16, 23]. The SCF, HCF, and PCF samples evidenced a shift of this band at higher wavenumber (1079, 1080, and 1085 cm^{-1}, respectively) that further increased for the *h*-SCF and *h*-HCF (1089 and 1088 cm^{-1}, respectively, data not shown for brevity). This shift may be ascribed to the change in the relative amounts of T–O–Si species [16], which takes place in alkaline solution. In details, the SiO_4 and AlO_4 units of the amorphous phases of silico-aluminate structure, in alkaline conditions, break and re-combine in species with a higher covalent connectivity inducing a shift of the T–O–Si bond toward higher wavenumber.

In addition, the SCF and HCF spectra displayed an absorbance peak around 735 cm^{-1} ascribed to intrinsic stretching vibrations of Al at the octahedral site (Al(6)), according to the geometrical configuration of nearest neighbors [16, 23].

This peak disappears after hydrothermal curing (*h*-SCF and *h*-HCF), due depolymerization of silico-aluminate species, Al(6), and structural amorphous reorganization of the same species, Al(4)) tetrahedral coordinated [23]. This behavior is not observed for the *h*-PCF.

These findings, confirmed by SEM results, suggest that the presence of Silicon metal in the SCF and HCF system enhances the formation of a geopolymeric network. The generation of hydrogen from the redox reaction between the Si powder and the alkaline solution was followed by the gelification of silicate and then by dissolution and formation of new silico-aluminate phases, which contributed to the hardening of the inorganic continuous phase.

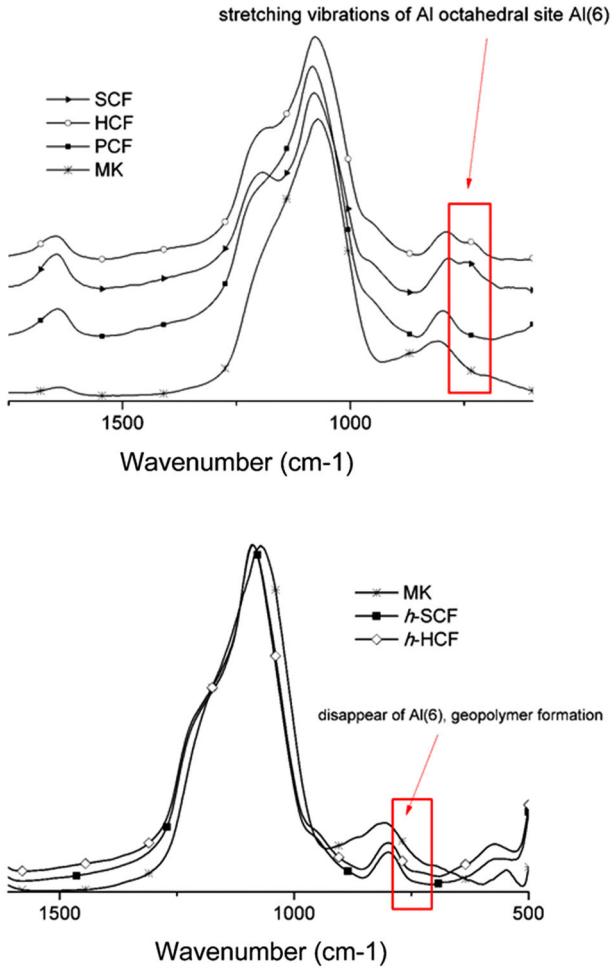

Fig. 3 FTIR investigation

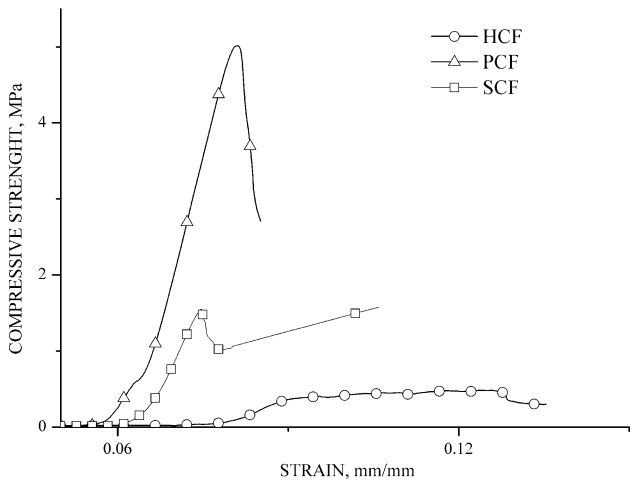

Fig. 4 Mechanical properties

Accordingly, the compressive strength data (reported in Fig. 4 and Table 2), highlighted that, for the SCF and HCF foams, the presence of the Si component strongly contributed to the consolidation of the inorganic structure providing higher mechanical performances [24].

Table 2 Mechanical characterization of the ceramic foams

Samples	Density (kg/m^3)	R_c (MPa)	R_f (MPa)
SCF	1000	4.62 ± 0.07	0.14 ± 0.01
HCF	450	1.41 ± 0.07	0.21 ± 0.01
PCF	290	0.49 ± 0.03	0.14 ± 0.01
CS[a]	1100	5.92 ± 0.07	1.30 ± 0.07

[a] Compact solid

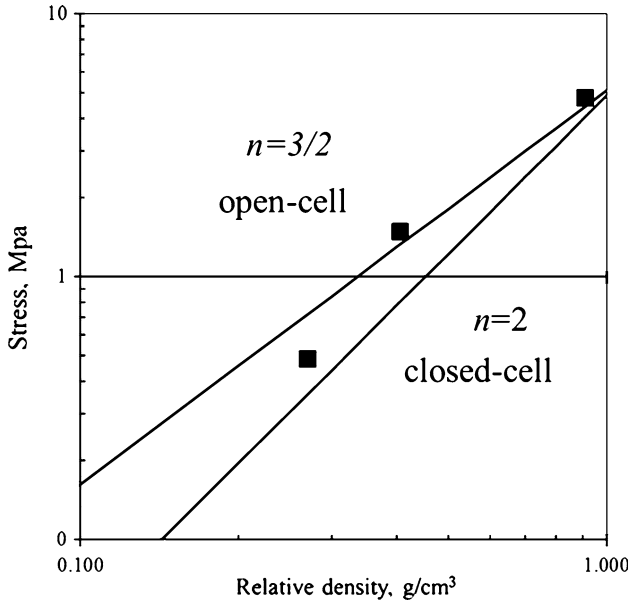

Fig. 5 Compression strength as a function of relative density

In addition, for HCF system, a toughness effect was also observed, because the presence of "meringue" foam acted not only as simple templating agent, but it contributed actively to stabilize the hybrid foam through the formation of a cross-linked organic network [10] chemically bonded to inorganic phase.

On the contrary, PCF foam showed very poor mechanical properties (see Table 2) due to a low extent of geopolymeric reactions. In fact, it is believed that the amount of un-reacted material acts as defect site and affects negatively the mechanical behavior [22].

As proposed by Gibson-Ashby [25], the relative strength of a cellular material is related to its relative density by the following equation:

$$\frac{\sigma_F^*}{\sigma_C} = C\left(\frac{\rho_F^*}{\rho_C}\right)^n,$$

where ρ_F* and σ_F* are the relative density and compressive strength of the ceramic foam, respectively. ρ_c and σ_C are referred to the compact solid. C is a dimensionless constant and the exponent n depending on the cell morphology.

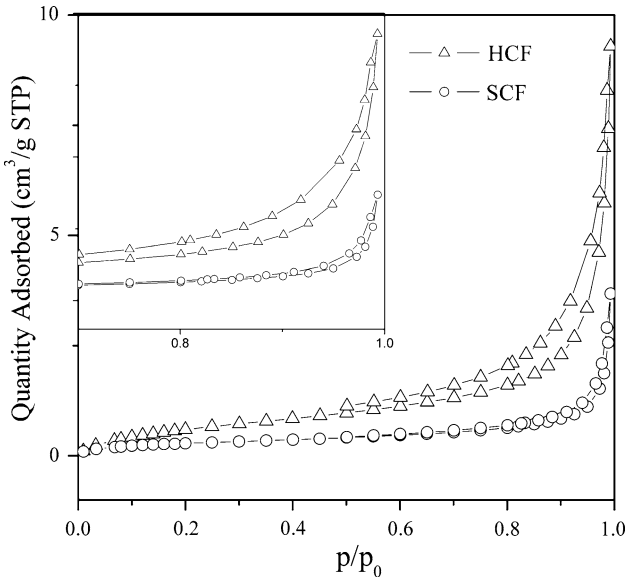

Fig. 6 N_2 adsorption/desorption isotherms of HCF and SCF samples

Figure 5 reports strength data as a function of the relative density and compares the foam behavior either with a completely open-cell or closed-cell foams. The lack of a perfect fit to Ashby's theory can be due to the presence of mixed closed and open cells. In fact, the hybrid ceramic foams are characterized by an interconnected porosity, where some pores are present in most of the cell walls [26, 27].

The results of N_2 adsorption/desorption measurements were reported in Fig. 6. The samples HCF and SCF showed low values of the BET surface area. In particular, the BET surface area was higher in HCF (2.614 m^2/g) compared to SCF (1.482 m^2/g) samples. Both isotherms belong to Type II from the IUPAC classification [28], characteristic of macroporous materials. Accordingly, with the SEM results, the HCF isotherm showed a narrow hysteresis loop, due to the more heterogeneous pore distribution of the hybrid foam. However, these BET values are fairly low when compared to other foams characterized by a higher degree of cell interconnections within the entire structure. This suggested that, even though an open-cell structure was observed by SEM, the cell interconnection was low in these foamed structures. Moreover, low values of specific surface area can be due to the presence of un-reacted silico-aluminate phase (also confirmed by SEM analysis, Fig. 2) which fills the mesopores of the partially polymerized foams [1, 24].

Conclusions

Hybrid foams based on geopolymeric matrix were engineered by employing different foaming methods. In the first method, gaseous hydrogen produced by the oxidization of Si powder in an alkaline media was used as blowing agent to generate gas bubbles in the geopolymeric matrix. In the second method, the porous structure was generated by mixing the paste with a "meringue" type of foam previously prepared by whipping, under vigorous stirring, a water solution containing vegetal proteins as surfactants. In the third method, a combination of these two methods was employed. In particular, we found that the combination of the "meringue" approach with the use of Silicon powder, as blowing agent, can lead to the formation of hybrid foams (HCF) having a geopolymeric structure bonded to an organic phase (protein). The whipped protein has the important role to stabilize the hybrid foam through the formation of a cross-linked organic network chemically bonded to inorganic phase. The synergistic effect of two different foaming agents leads to an interconnected porosity and low density. At the same time, it is possible to obtain a product with mechanical properties mediated between ceramic and polymeric foams.

Acknowledgements This work was supported by the Italian Ministero dell'Istruzione, dell'Università e della Ricerca (MIUR), and Ministero dello Sviluppo Economico within the framework of PON-2007-2013 under Grant PON02_000293206086 "COCET". The authors gratefully acknowledge Dott. Manlio Colella for helping in analyzing SEM microscopy data.

References

1. Landi E, Medri V, Papa E, Dedecek J, Klein P, Benito P, Vaccari A (2013) Alkali-bonded ceramics with hierarchical tailored porosity. Appl Clay Sci 73:56–64
2. Kamseu E, Nait-Ali B, Bignozzi MC, Leonelli C, Rossignol S, Smith DS (2012) Bulk composition and microstructure dependence of effective thermal conductivity of porous inorganic polymer cements. J Eur Ceram Soc 32(8):1593–1603
3. Duxson P, Fernández-Jiménez A, Provis JL, Lukey GC, Palomo A, van Deventer JSJ (2007) Geopolymer technology: the current state of the art. J Mater Sci 42(9):2917–2933. doi:10.1007/s10853-006-0637-z
4. Van Bonin W, Nehen U, Von Gizycki U (1975) Hydrogen peroxides blowing agent for silicate foams. US Patent 3,864,137
5. Vaou V, Panias D (2010) Thermal insulating foamy geopolymers from perlite. Miner Eng 23:1146–1151
6. Prud'Homme E, Michaud P, Joussein E, Peyratout C, Smith A, Rossignol S (2011) *In situ* inorganic foams prepared from various clays at low temperature. Appl Clay Sci 51(1):15–22
7. Studart AR, Gonzenbach UT, Tervoort E, Gauckler LJ (2006) Processing routes to macroporous ceramics: a review. J Am Ceram Soc 89(6):1771–1789
8. Colombo P, Vakifahmetoglu C, Costacurta S (2010) Fabrication of ceramic with hierarchical porosity. J Mater Sci 45:5424–5455. doi:10.1007/s10853-010-4708-9
9. Scheffler M, Colombo P (2005) Cellular ceramics: structure, manufacturing, properties and applications. Wiley–VCH Verlag GmbH, Weinheim, Germany
10. Lyckfeldt O, Brandt J, Lesca S (2000) Protein forming—a novel shaping technique for ceramics. J Eur Ceram Soc 20(14):2551–2559
11. Garrn I, Reetz C, Brandes N, Kroh LW, Schubert H (2004) Clot-forming: the use of proteins as binders for producing ceramic foams. J Eur Ceram Soc 24(3):579–587

12. Murray BS, Ettelaie R (2004) Foam stability: proteins and nanoparticles. Curr Opin Colloid In 9(5):314–320
13. Bos MA, Van Vliet T (2001) Interfacial rheological properties of adsorbed protein layers and surfactants: a review. Adv Colloid Interfac 91(3):437–471
14. Damodaran S (2005) Protein stabilization of emulsions and foams. J Food Sci 70(3):54–66
15. Chen J, Dickinson E (1998) Viscoelastic properties of protein-stabilized emulsions: effect of protein-surfactant interactions. J Agr Food Chem 46(1):91–97
16. Verdolotti L, Di Maio E, Forte G, Lavorgna M, Iannace S (2010) Hydration-induced reinforcement of polyurethane–cement foams: solvent resistance and mechanical properties. J Mater Sci 45(12):3388–3391. doi:10.1007/s10853-010-4416-5
17. Xu H, Van Deventer JSJ (2000) The geopolymerisation of alumino-silicate minerals. Int J Miner Process 59(3):247–266
18. Wang L, Tomura S, Suzuki M, Ohashi F, Inukai K, Maeda M (2001) Synthesis of mesoporous silica material with sodium hexafluorosilicate as silicon source under ultra-low surfactant concentration. J Mater Sci Lett 20:277–280
19. Zhang XG (2001) Elettrochemistry of silicon and its oxides. Kluver Academic/Plenum Publisher, New York
20. Mo BH, Zhu H, Cui XM, He Y, Gong SY (2014) Effect of curing temperature on geopolymerization of metakaolin-based geopolymers. Appl Clay Sci 99:144–148
21. Xu H, van Deventer JS (2003) The effect of alkali metals on the formation of geopolymeric gels from alkali-feldspars. Colloid Surface A 216(1):27–44
22. Komnitsas K, Zaharaki D (2007) Geopolymerisation: a review and prospects for the minerals industry. Miner Eng 20(14): 1261–1277
23. Davidovits J (1991) Geopolymers. J Therm Anal Calorim 37(8):1633–1656
24. Medri V, Papa E, Dedecek J, Jirglova H, Benito P, Vaccari A, Landi E (2013) Effect of metallic Si addition on polymerization degree of in situ foamed alkali-aluminosilicates. Ceram Int 39(7):7657–7668
25. Gibson LJ, Ashby MF (1999) Cellular solids: structure and properties. Cambridge University Press, Cambridge, MA
26. Colombo P, Hellmann JR, Shelleman DL (2001) Mechanical properties of silicon oxycarbide ceramic foams. J Am Ceram Soc 84(10):2245–2251
27. Hung TC, Huang JS, Wang YW, Fan YC (2013) Microstructure and properties of metakaolin-based inorganic polymer foams. J Mater Sci 48(21):7446–7455. doi:10.1007/s10853-013-7559-3
28. Sing KSW, Everett DH, Haul RAW, Moscou L, Pierotti RA, Rouquerol J (1985) Pure Appl Chem 57:603–619